Journal of Environmental Management 210 (2018) 226–238

Contents lists available at ScienceDirect

Journal of Environmental Management

journal homepage: www.elsevier.com/locate/jenvman

Research article

Efficient removal of Acid Green 25 dye from wastewater using activated *Prunus Dulcis* as biosorbent: Batch and column studies

Suyog N. Jain, Parag R. Gogate*

Chemical Engineering Department, Institute of Chemical Technology, Nathalal Parekh Marg, Matunga, Mumbai 400019, India

ARTICLE INFO

Article history:
Received 18 October 2017
Received in revised form
28 December 2017
Accepted 4 January 2018

Keywords:
Adsorption
Dye removal
Batch study
Column study
Kinetics
Reusability

ABSTRACT

Biosorbent synthesized from dead leaves of *Prunus Dulcis* with chemical activation during the synthesis was applied for the removal of Acid Green 25 dye from wastewater. The obtained biosorbent was characterized using Brunauer-Emmett-Teller analysis, Fourier transform-infrared spectroscopy and scanning electron microscopy measurements. It was demonstrated that alkali treatment during the synthesis significantly increased surface area of biosorbent from 67.205 to 426.346 m^2/g. The effect of various operating parameters on dye removal was investigated in batch operation and optimum values of parameters were established as pH of 2, 14 g/L as the dose of natural biosorbent and 6 g/L as the dose of alkali treated biosorbent. Relative error values were determined to check fitting of obtained data to the different kinetic and isotherm models. It was established that pseudo-second order kinetic model and Langmuir isotherm fitted suitably to the obtained batch experimental data. Maximum biosorption capacity values were estimated as 22.68 and 50.79 mg/g for natural biosorbent and for alkali activated *Prunus Dulcis*, respectively. Adsorption was observed as endothermic and activation energy of 6.22 kJ/mol confirmed physical type of adsorption. Column experiments were also conducted to probe the effectiveness of biosorbent for practical applications in continuous operation. Breakthrough parameters were established by studying the effect of biosorbent height, flow rate of dye solution and initial dye concentration on the extent of dye removal. The maximum biosorption capacity under optimized conditions in the column operation was estimated as 28.57 mg/g. Thomas and Yoon-Nelson models were found to be suitably fitted to obtained column data. Reusability study carried out in batch and continuous column operations confirmed that synthesized biosorbent can be used repeatedly for dye removal from wastewater.

1. Introduction

Dyes are color bearing organic compounds which are used to apply color to various substrates such as textile materials, paper, cosmetics and plastics. Dyes impart color to substrate by binding themselves to fabrics or surfaces (Ngulube et al., 2017). Dye uses as colorant in different industries like textile, paper, plastic, etc. are increasing worldwide. About 56% of the annual worldwide production of the total synthetic dyes is consumed by textile industries. During the process of dye production and also dyeing, a large quantity of dye is released/lost into the effluent due to improper handling and/or incomplete dye fixation onto the fabric. Dyes are recalcitrant and stable towards the environment and thus are harmful to human being and living species including microorganisms (Moussavi and Khosravi, 2011). Some of the dyes are also carcinogenic and teratogenic offering significant risk to the aquatic species and human beings (Song et al., 2017). Presence of dyes in the effluents also reduces the photosynthetic activity of aquatic plants and thus disturbs the equilibrium of nature. Dyes also impart bad taste and give significant odor to water bodies (Santos et al., 2017; Subramaniam and Ponnusamy, 2015). Severe health disorders in terms of dysfunction of liver, kidney and nervous system can be caused by dyes (Zhou et al., 2015). Discharge of dye effluents directly into the water bodies can affect the health of the people who are using this water for drinking purpose (Adegoke and Bello, 2015). Dye removal from effluents is a major problem faced by textile industries. It is challenging to address the environmental issues created by dye effluents and in this regard, there is a need to develop effective treatment methods to destroy or isolate the dyes from the effluents before discharge into the water bodies to protect

* Corresponding author.
E-mail address: pr.gogate@ictmumbai.edu.in (P.R. Gogate).

https://doi.org/10.1016/j.jenvman.2018.01.008
0301-4797/

ecosystem.

Several physical methods such as ultrafiltration (Ng et al., 2017), electrodialysis (Xue et al., 2015), reverse osmosis (Nataraj et al., 2009) and chemical methods such as electroflotation (Balla et al., 2010) and electrochemical oxidation (Singh et al., 2016) have been applied by researchers for dye removal from aqueous solution. However these treatment methods are not found to be cost effective and also some of these treatment techniques involve use of excessive chemicals which also create additional environmental concerns (Demirbas, 2009). These limitations may be overcome by the method of adsorption. In adsorption, activated carbon is commonly used for dye removal due to its effectiveness, but this offers drawbacks of high cost of the treatment process, difficulty in regeneration after exhaustion during the use and reduced adsorption efficiency after regeneration (Srivastava et al., 2007). Hence research into development of low cost, sustainable and efficient adsorbent for dye removal is on the forefront in recent years. Different adsorbents in their natural form such as *Xanthium strumarium* L. seed hull (Khamparia and Jaspal, 2017), bagasse fly ash (Mall et al., 2005), coconut mesocarp (Monteiro et al., 2017) as well as in the activated form such as oxalic acid treated *Artocarpus odoratissimus* peel (Dahri et al., 2017), surfactant treated saponite (Tangaraj et al., 2017) and H_3PO_4 activated cattail (Shi et al., 2010) have been utilized for removal of dyes from wastewater. In the present study, removal of Acid Green 25 (AG 25) dye has been studied using biosorbent synthesized from dead (fallen) leaves of *Prunus Dulcis* (PD) in raw form and using NaOH (alkali) treatment during the synthesis. The literature analysis established that utilization of dead leaves of *Prunus Dulcis* (DLPD) has not been explored for the biosorbent synthesis and application for AG 25 dye removal from wastewater. The advantage of biosorbent selected in the present study in comparison with other biosorbents is its availability in large quantity at minimal cost, especially in the agriculture dominated countries. Also the use of such agricultural waste (biomass) as a biosorbent can reduce the volume of solid waste as it follows the principle of wealth from waste. AG 25, an organic sulphonic acid dye, selected as pollutant in the present study finds applications in textile, leather and cosmetic industry. AG 25 dye containing effluent can cause eye and skin irritation and also the compound is toxic to aquatic organisms. Hence removal of AG 25 dye from wastewater is necessary to protect the ecosystem and there is always a need to develop effective and economical treatment approaches. In present study, batch experiments have been carried out initially to investigate the effect of operating parameters on dye removal. The industrial processes of adsorption typically need to be conducted in column mode due to the large volumes of the effluent to be handled and hence column experiments have also been conducted to probe the effectiveness of synthesized NaOH activated *Prunus Dulcis* (NAPD) for operation in continuous manner. The effect of operating parameters in the column operation on AG 25 dye removal was also investigated to establish breakthrough conditions, which are important design parameters.

2. Materials and methods

2.1. Biosorbent synthesis

Dead (fallen) leaves of *Prunus Dulcis* (DLPD) were collected, washed, dried and crushed. The obtained powder was screened in sieve shaker to get particles in the size range of 53–106 μm. The obtained biosorbent was used as such in the natural form and also subjected to activation. In the process of activation, Lignin from the powder (DLPD) was removed by activation of powder with NaOH solution. 1 part of obtained powder was treated with 5 parts of NaOH solution (1% by weight) for 4 h in a reactor at temperature of 323 K. The mixture was then filtered, washed with distilled water for removing colored lignin and then again heated at 323 K in oven. The synthesized NaOH activated *Prunus Dulcis* (NAPD) biosorbent in this manner was then stored in glass bottles to be used for further studies.

2.2. Pollutant dye

An anionic dye, Acid Green 25 [Molecular formula = $C_{28}H_{20}N_2Na_2O_8S_2$, molecular weight = 622.57 g/mol], was obtained from Sigma-Aldrich, India. 1000 mg/L of stock dye solution was prepared and then diluted to obtain desired dye solutions required for batch and column study.

2.3. Biosorbent characterization

Scanning electron microscopy (SEM, JEOL 6380, USA) was used to examine surface morphology of NAPD biosorbent before and after the adsorption of AG 25 dye as well as of the natural form of DLPD. The functional groups involved in the process of AG 25 dye adsorption on synthesized NAPD biosorbent were analyzed using Fourier transform-infrared spectroscopy (FT-IR, Perkin Elmer BX, USA). BET parameters for the DLPD and NAPD biosorbents were evaluated using the Brunauer-Emmett-Teller (PMI BET Sorptometer-201AEL-2OSEL, USA) method. UV Spectrophotometer (Shimadzu-1800, Japan) was used for determining the concentration of AG 25 dye in the solution by recording the UV absorbance at λ_{max} of 642 nm. Limit of detection and limit of quantification, which are the validation parameters for data were also evaluated as 0.0995 and 0.3318 mg/L respectively.

2.4. Batch equilibrium studies

Batch equilibrium studies were performed in orbital shaker (Bio-Technics, Mumbai). Desired amount of synthesized biosorbent was added in 50 mL of aqueous solution of AG 25 dye having a specific concentration and at the desired pH value. The pH of the dye solution was adjusted to the required value by adding 0.1 N HCl/0.1 N NaOH as required for pH adjustment. The shaking was performed at constant speed of 150 rpm. The effect of operating parameters like pH of dye solution, biosorbent loading, time, AG 25 dye concentration and temperature on the extent of dye removal have been investigated. Samples were withdrawn from the shaker at specific time intervals and analyzed using UV spectrophotometer. Reusability study of the biosorbent was also performed by first desorbing AG 25 dye from NAPD biosorbent based on the regeneration approach and reusing the biosorbent again in the study. Dye loaded NAPD biosorbent was thoroughly mixed with 0.1 mol/L NaOH solution applied as a desorbing agent (Guo et al., 2012) in orbital shaker. After desorption, reusability of the recovered biosorbent was further checked in five consecutive cycles.

Biosorption capacity (q_t) defined as ratio of dye adsorbed (mg) to biosorbent mass (g) was estimated using the equation given below:

$$q_t = \frac{(C_i - C_t)}{m} \quad (1)$$

where C_i and C_t (mg/L) are initial concentration and concentration at any time, t of AG 25 dye in the solution, respectively and m is biosorbent load (g/L).

The extent of dye removal (%) was evaluated using equation as given below:

$$\textit{Extent of removal}(\%) = \frac{C_i - C_t}{C_i} \times 100 \quad (2)$$

2.5. Column biosorption study

Column biosorption experiments were also carried out in a glass column of 2 cm inner diameter and height of 25 cm. The setup was equipped with peristaltic pump (Ravel Hiteks, India) for recirculation. Glass wool packing was provided in the column to avoid the biosorbent loss during the operation and glass beads were used to support the bed. AG 25 dye solution of required concentrations was pumped upward through the biosorbent bed at required flow rate. The residual concentration of dye in the effluent samples was determined using UV- visible spectrophotometer analysis by collecting the effluent samples from top of the column at required time intervals. The effect of different operating parameters like biosorbent height, flow rate of dye solution and initial AG 25 dye concentration on the dye removal rate was studied and different breakthrough conditions were then established from the data analysis. Breakthrough plots of *Ct/Ci* versus time were obtained for different sets of column parameters and obtained data were analyzed by applying the various column models.

Breakthrough time (t_b) is the time required for the concentration in the effluent stream to reach to 5–10% of the feed concentration (Souza et al., 2008). In present study, t_b was determined when effluent stream dye concentration reached to 10% of the feed concentration. The exhaustion time (t_{eff}) was measured as the time when dye concentration in the effluent stream reaches 90% of the feed concentration (Wu et al., 2012).

The treated effluent volume, V_{eff} (L) was estimated by using the following equation (Singh et al., 2017a):

$$V_{eff} = Qt_{eff} \tag{3}$$

where Q is the flow rate at which dye solution passes through the column (mL/min).

The maximum (experimental) uptake capacity, q_m (mg/g), defined as ratio of mass of dye adsorbed (q_a) to the biosorbent mass in the column (W) was estimated using the equation given below (Yusuf et al., 2017):

$$q_m = \frac{q_a}{W} \tag{4}$$

In addition, the value of q_m was also determined using the mathematical models based to establish the best fitting. Extent of desorption (%) was also estimated as ratio of mass of dye desorbed (q_d, mg) during the regeneration process to the mass of dye adsorbed (q_a, mg) (Singh and Shukla, 2016):

$$\textit{Extent of Desorption}(\%) = \frac{q_d}{q_a} \times 100 \tag{5}$$

3. Results and discussion

3.1. Biosorbent characterization

Scanning electron microscopy images of DLPD, NAPD before and after AG 25 dye adsorption have been depicted in Fig. 1a–c respectively. It can be predicted from Fig. 1b that NAPD biosorbent has irregular and significant number of cavities/pores where AG 25 dye molecules can get accumulated. DLPD has relatively lower fraction of irregular structures including the pores. Image in Fig. 1c is found to be altered morphologically which can be attributed to adsorption of dye on the NAPD surface, leading to blocking of pores.

The obtained results of FTIR analysis of NAPD before and after AG 25 dye adsorption are depicted in Fig. 2a and b, respectively. The broad peak at 3347 cm^{-1} (Fig. 2a) corresponds to OH and NH group stretching vibration (Almasian et al., 2016) which shifted to 3354 cm^{-1} (Fig. 2b) after AG 25 dye adsorption. The band at 2924 cm^{-1} is attributed to CH group in cellulose (Singh et al., 2017b; Zeng et al., 2017) of NAPD as seen in both the figures. The strong band at 1616 cm^{-1} corresponding to CO stretching (Jia et al., 2017; Sidiras et al., 2011) in Fig. 2a shifted to 1612 cm^{-1} after AG 25 dye adsorption. The peak at 1319 cm^{-1} corresponding to CN stretch (Pereira et al., 2017) observed in the native biosorbent shifted to 1326 cm^{-1} after AG 25 dye adsorption. The occurrence of new band at 1180 cm^{-1} in Fig. 2b corresponds to SO_3 group (Pachhade et al., 2009; Wu et al., 2015) of AG 25 dye which confirmed the adsorption of AG 25 dye on NAPD biosorbent.

The obtained data for the BET specific surface area, mean pore diameter and pore volume of DLPD and NAPD are shown in Table 1. Specific surface area of DLPD was estimated as 67.205 m^2/g whereas the NaOH treatment increased surface area to 426.346 m^2/g as observed in the case of NAPD. Pore diameter obtained in the case of DLPD was 3.713 nm which reduced to 2.644 nm in the NAPD due to NaOH treatment. Pore volume of DLPD was obtained as 0.062 cm^3/g. NaOH treatment increased pore volume to 0.282 cm^3/g as observed in the case of NAPD. Significant increase in surface area and pore volume for NAPD as compared to DLPD can be attributed to removal of lignin from dead leaves of PD due to NaOH treatment, leading to development of pores and hence an increase in the surface area and pore volume.

The zero point charge (pH_{zpc}) is the value of pH at which NAPD biosorbent carries neutral charge. pH_{zpc} was estimated using method described by Prahas et al. (2008). pH_{zpc} value for NAPD was estimated to be 6.27.

3.2. Batch Study

3.2.1. Effect of pH

Fig. 3 depicts the obtained results for the effect of pH on AG 25 dye removal. When pH of the AG 25 dye solution increased from 2 to 10, the dye removal efficiency decreased from 91.04 to 21.69% for

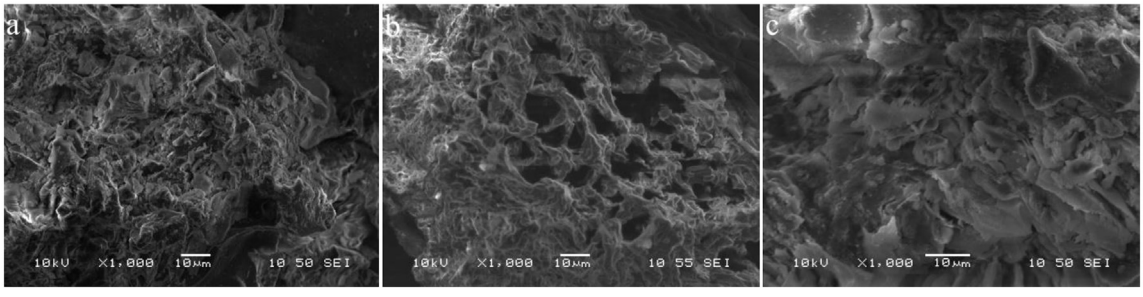

Fig. 1. Scanning electron microscopy images of biosorbents (a) DLPD (b) NAPD before AG 25 dye adsorption (c) NAPD after AG 25 dye adsorption.

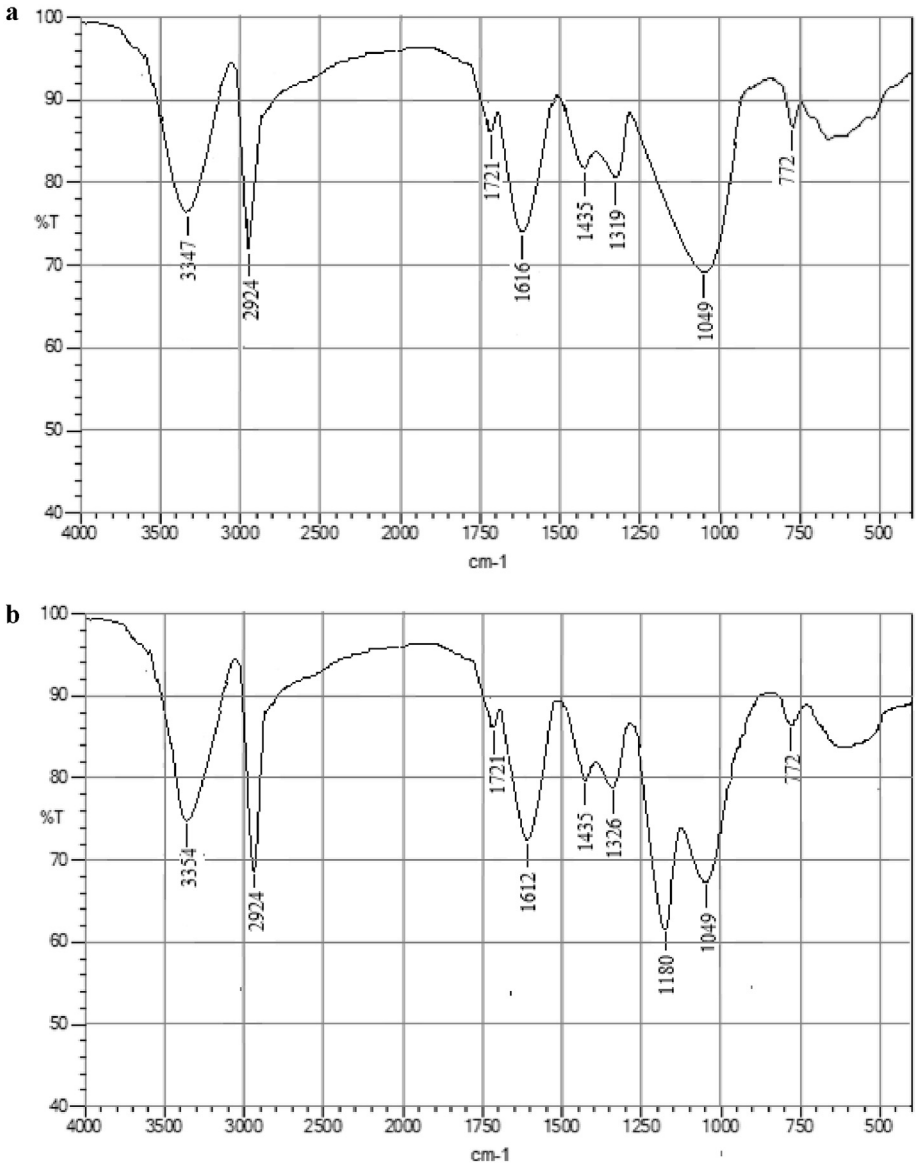

Fig. 2. FT-IR spectra of NAPD (a) before AG 25 dye adsorption (b) after AG 25 dye adsorption.

Table 1
BET surface area, pore diameter and pore volume of DLPD and NAPD.

Biosorbent sample	Specific surface area (m^2/g)	Pore diameter (nm)	Pore volume (cm^3/g)
DLPD	67.025	3.713	0.062
NAPD	426.346	2.644	0.282

the case of NAPD biosorbent whereas it decreased from 82.61 to 10.87% for the case of DLPD biosorbent. Biosorption capacity also decreased for both the biosorbents with an increase in pH of the dye solution. Maximum dye removal and biosorption capacity was achieved at pH of 2, which can be attributed to the fact that at pH of 2, significant force of attraction exists between negative sulfonic group present on AG 25 dye and positive charge on NAPD surface due to an increase in concentration of positive (H^+) cations at pH of 2 (acidic conditions) giving maximum dye removal (Hameed et al., 2007). Similar trend was also observed for Acid Red 57 removal using surfactant treated sepiolite (Ozcan and Ozcan, 2005). In the present work, pH_{zpc} value for NAPD was estimated to be 6.27, which also confirms that positive charge will be developed on the surface of NAPD at pH values less than pH_{zpc} driving enhanced removal of acidic AG 25 dye. The pH of 2, which was established to give maximum removal, was subsequently used for the further batch as well as column studies.

3.2.2. *Effect of biosorbent dosage (m)*

The effect of both DLPD (over the range of 1–20 g/L) and NAPD (over the range of 0.5–10 g/L) biosorbent dosage on the adsorption of AG 25 dye was also investigated and the obtained results have been depicted in Fig. 4. The extent of removal of AG 25 dye was found to significantly increase from 10.78% at 1 g/L to 82.61% at 14 g/L loading of DLPD and from 27.11% at 0.5 g/L to 91.04% at 6 g/L loading for the case of NAPD. Beyond these loading of 14 g/L and 6 g/L established as optimum for the case of DLPD and NAPD respectively, there was only a marginal change in extent of removal with a further increase in the biosorbent loading. The obtained results also established improved dye removal at lower biosorbent dosage for NAPD than DLPD, which can be attributed to more

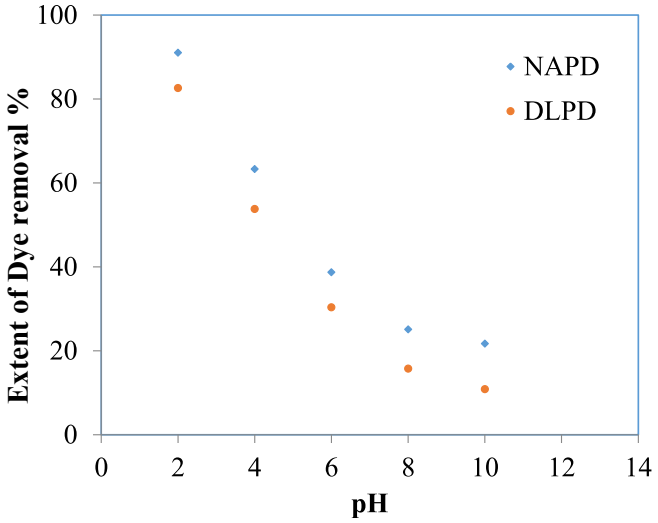

Fig. 3. Effect of pH on extent of AG 25 dye removal using DLPD and NAPD.

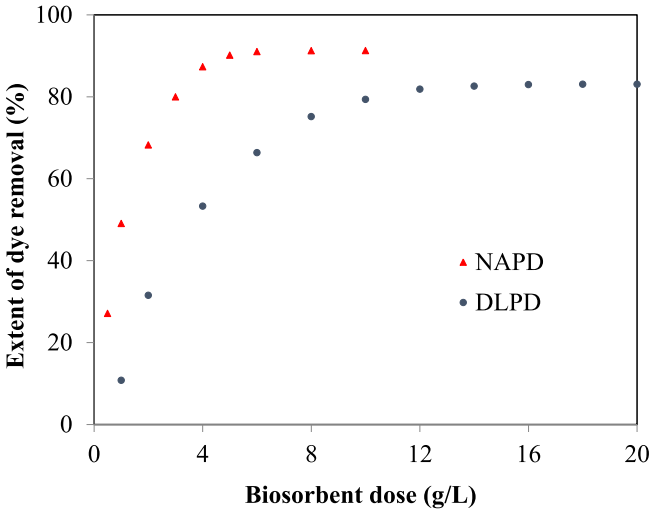

Fig. 4. Effect of biosorbent dose on the removal of AG 25 dye using DLPD and NAPD.

surface area being available for dye adsorption in the case of NAPD (Table 1). The increase in dye removal with biosorbent dosage till the optimum for both the types of biosorbents can be due to easy accessibility of more number of vacant sites at higher dosage on the biosorbent surfaces (Gündüz and Bayrak, 2017). After the optimum biosorbent dosage of 14 g/L for the DLPD and 6 g/L for the NAPD, marginal variation in removal efficiencies can be attributed to aggregation of particles occurring at higher biosorbent causing a decrease in biosorbent surface area (Ozacar and Ayhan Sengil, 2005). Considering these results, the further batch study was performed at loading of 14 g/L for the DLPD and 6 g/L for the NAPD.

Increase in biosorbent loading also caused significant decrease in q_t from 10.78 mg/g at 1 g/L to 5.9 mg/g at 14 g/L for the case of DLPD and from 54.21 mg/g at 0.5 g/L to 15.17 mg/g at 6 g/L for the case of NAPD. It is important that maximum removal of dye can be achieved in an efficient manner and hence selection of optimum loading is important. The observed trend of increase in dye removal and decrease in q_t with an increase in biosorbent dosage till the optimum is also confirmed from reported trend for methylene blue dye removal using the peel waste of *cucumis sativus* (Shakoor and Nasar, 2017) and rhodamine 6G dye removal using Moroccan natural phosphate (Bensalah et al., 2017). It is also important to note that the established optimum loading is different depending on the pollutant and specific system used for adsorption. Optimum dose of 4 g/L was reported for methylene blue dye removal using peel waste of *cucumis sativus* whereas optimum of 20 g/L was reported for rhodamine 6G dye removal using Moroccan natural phosphate. Thus, it is important to study the effect of loading of the specific biosorbent for each pollutant in question and hence the importance of the present work is clearly established.

3.2.3. Effect of contact time (t) and dye concentration (C_i)

The time dependency of the biosorption of AG 25 on NAPD was investigated for different dye concentrations over the range of 50 to 200 mg/L and obtained results are shown in Fig. 5. In the first 30 min of operation for all AG 25 dye concentrations studied in the present work, it was observed that approximately 50% of the dye removal occurred and subsequently till the treatment period of 120 min, maximum dye removal occurred. Finally the time profile indicated that saturation was achieved by treatment time of 330 min. The maximum dye removal in initial periods is due to availability of maximum number of active sites for the dye adsorption, and the dye removal later slows down gradually due to reduction in the available sites for adsorption based on the occupancy. Similar trend was also reported for adsorption of Acid Blue 25 dye on activated *Ficus racemosa* (Jain and Gogate, 2017). Beyond 330 min as the treatment time, dye removal was mostly constant which can be attributed to the attainment of equilibrium (Bhattacharyya et al., 2017). Hence, all the further batch experiments were carried out for time of 330 min.

The effect of AG 25 dye concentration on extent of dye removal and biosorption capacity has also been depicted in Fig. 5. The biosorption capacity increased from 8.01 mg/g at 50 mg/L as the initial AG 25 dye concentration to 27.52 mg/g at 200 mg/L of AG 25 concentration. The increase in AG 25 dye concentration enhanced the interaction forces required to overcome the resistance associated with mass transfer between dye and biosorbent giving higher biosorption capacity values. Similar trend was also reported for Bezathren dyes removal using sodic bentonite (Belbachir and Makhoukhi, 2017) and for the adsorption of Acid red 18 on activated natural zeolite (Mirzaei et al., 2017).

It was also observed that the extent of AG 25 removal decreased from 96.1% at 50 mg/L to 82.03% for 200 mg/L of concentration. Higher extent of dye removal at lower AG 25 dye concentration can be attributed to maximum probability of binding of all molecules of

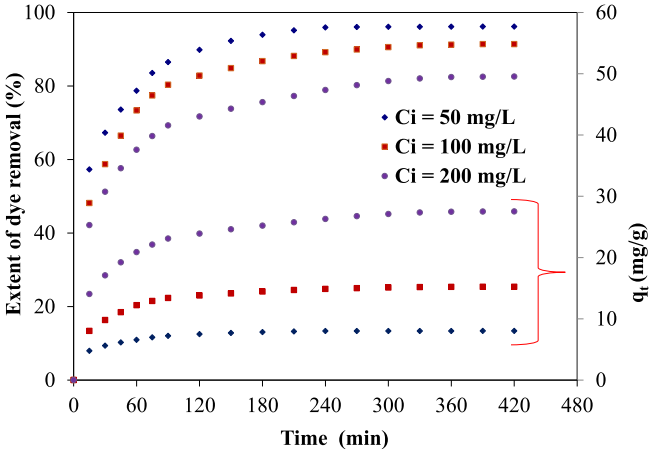

Fig. 5. Effect of contact time and initial dye concentration on biosorption capacity of NAPD and the extent of removal of AG 25 dye.

dye to the biosorption sites at lower concentration, which cannot be the case for higher AG 25 dye concentration as the available sites are fixed (Chowdhury et al., 2011). Similar trend was also reported for tartrazine dye removal using saw dust based biosorbent (Banerjee and Chattopadhyaya, 2017). It is important to note that though the extent of removal is higher at lower concentrations, the actual operation will depend on the available concentration in the effluent stream as it may not be feasible to lower the concentration by dilution due to the increased volumes to be treated on dilution.

3.2.4. Kinetic study

The obtained experimental data in the present study for AG 25 dye removal using NAPD were fitted to different kinetic models. Nonlinear regression analysis was performed to estimate the kinetic model parameters.

3.2.4.1. Lagergren pseudo first-order model. Pseudo first-order model is based on the mechanism that occupation rate of adsorption sites is proportional to quantum of free sites available for the adsorption. The nonlinear form of Lagergren pseudo first-order equation is given as follows (Lagergren, 1898):

$$q_t = q_e\left(1 - e^{-k_1 t}\right) \tag{6}$$

where, q_e is equilibrium sorption capacity (mg/g) and k_1 is Lagergren rate constant (min^{-1}).

The obtained pseudo first-order kinetic parameters (k_1 and q_e) for different sets of experiments are summarized in Table 2. It can be seen from Table 2 that the correlation coefficient, R^2 values (average value 0.8554) are significantly deviating from unity. The comparison of experimental (q_{exp}) and calculated (q_{cal}) values of biosorption capacities from kinetic models has also been shown in Fig. 6. It can be seen from Fig. 6 that calculated values of biosorption capacity (q_{cal}) using the pseudo first order model are deviating from the experimental values (q_{exp}). The results confirmed that pseudo first-order equation did not explain the obtained experimental data properly. The results regarding the suitability cannot be generalized as in the literature there have been some examples of better fitting such as for the case of the adsorption of safranin dye on activated corncob (Preethi et al., 2006). For the specific systems, experimental investigations and fitting of the model is always recommended as per the methodology described in the present work.

Table 2
Kinetic parameters for the removal of AG 25 dye using NAPD ($T = 303$ K, $t = 330$ min, pH = 2, $m = 6$ g/L).

Kinetic model	Parameter	Values		
Pseudo first- order	C_i (mg/L)	50	100	200
	Equilibrium q_{exp} (mg/g)	8.01	15.23	27.52
	Equilibrium q_{cal} (mg/g)	7.79	14.69	26.13
	k_1 (min^{-1})	0.042	0.035	0.032
	R^2	0.8268	0.8905	0.8488
Pseudo second-order	C_i (mg/L)	50	100	200
	Equilibrium q_{exp} (mg/g)	8.01	15.23	27.52
	Equilibrium q_{cal} (mg/g)	8.32	15.87	28.44
	k_2 (g mg^{-1} min^{-1})	0.0089	0.0037	0.0018
	R^2	0.9772	0.9902	0.9776
Fractional power law	C_i (mg/L)	50	100	200
	a (mg g^{-1} min^{-b})	3.73	6.14	9.90
	b	0.1351	0.1588	0.1762
	R^2	0.9041	0.9124	0.9569
Weber-Morris	C_i (mg/L)	50	100	200
First step	k_{ip} (mg g^{-1} $min^{-1/2}$)	0.43	1.08	1.62
	C (mg/g)	3.17	3.85	8.08
	R^2	0.9951	0.9999	0.9936
Second step	k_{ip} (mg g^{-1} $min^{-1/2}$)	0.05	0.28	0.51
	C (mg/g)	7.14	10.68	18.37
	R^2	0.7286	0.9785	0.9988
Third step	k_{ip} (mg g^{-1} $min^{-1/2}$)	–	0.06	0.07
	C (mg/g)	–	14.06	26.08
	R^2	–	0.8670	0.8292

3.2.4.2. Pseudo second-order model. Pseudo second-order model is based on the principle that rate of occupation of adsorption sites is proportional to the square of amount of the free sites. The nonlinear form of pseudo second-order equation is given as follows (Ho and Mckay, 1999):

$$q_t = \frac{q_e^2 k_2 t}{1 + k_2 q_e t} \tag{7}$$

where k_2 is pseudo second-order rate constant (g mg^{-1} min^{-1}).

The obtained pseudo second-order kinetic parameters (k_2 and q_e) are summarized in Table 2. It can be seen from Table 2 that the R^2 values (average value 0.9817) are closer to unity. It can also be seen from Fig. 6 that calculated values of biosorption capacity using the pseudo second order model are closer to the experimental values at different times and also equilibrium. The obtained results established that pseudo second-order equation fitted well to the obtained data. Similar fitting of second order has also been reported for the adsorption of AG 25 on polyaniline composite (Ayad and El-Nasr, 2012) and for the adsorption of methylene blue using activated coconut shell (Islam et al., 2017).

3.2.4.3. Fractional power model. The nonlinear form of fractional power model is given as follows (Bharathi and Ramesh, 2013):

$$q_t = at^b \tag{8}$$

where a (mg g^{-1} min^{-b}) and b (dimensionless) are the constants of the model.

The obtained fractional power model kinetic parameters (a and b) are summarized in Table 2. It can be seen from Table 2 that the R^2 values (average value 0.9245) are significantly deviating from unity. It can also be seen from Fig. 6 that calculated values of biosorption capacity using the fractional power model are deviating from the experimental values under all the conditions. The obtained finding indicated that fractional power kinetic model did not explain the obtained data properly. Similar nature was also observed for Rhodamine dye removal using biosorbent based on fruit epicarp of *Raphia hookerie* (Inyinbor et al., 2016).

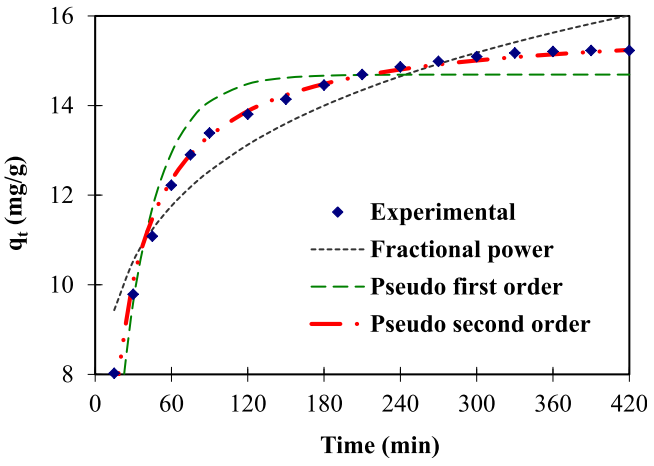

Fig. 6. Comparison of q_t calculated from different kinetic models with experimental for the removal of AG 25 using NAPD at initial dye concentration of 100 mg/L.

3.2.4.4. Weber-Morris model. It is necessary to predict the rate controlling step in the adsorption as this is a useful information for design. The obtained kinetic data in the adsorption was analyzed using Weber-Morris diffusion model to determine the adsorption mechanism and the controlling step. The model is expressed by the following equation (Weber and Morris, 1963):

$$q_t = k_{ip}\sqrt{t} + C \tag{9}$$

where k_{ip} is the diffusion rate constant (mg g^{-1} $min^{-1/2}$) and C is the constant (mg/g) quantifying the boundary layer thickness and these model parameters can be obtained from the slope and intercept of the linear plot of q_t versus $\sqrt{t}$. Fig. 7 shows the depiction of the fitting of the Weber-Morris model to the obtained data and obtained results for parameters are summarized in Table 2. Linear lines passing through the origin were not obtained for any of the dye concentrations, which confirmed that intra-particle diffusion is only one of the steps but not the only controlling step in deciding the efficacy of adsorption (Ma et al., 2017). It can be also established from Fig. 7 that biosorption of AG 25 on NAPD is a multistep process consisting of first step as external diffusion of AG 25 dye on NAPD surface, second step as dye diffusion into the NAPD pores (intra-particle diffusion) and third step of actual adsorption driven by equilibrium (especially at higher concentrations greater than 100 mg/L, for lower concentration of 50 mg/L, only two steps are observed and hence Table 2 also gives data for two steps only for the lower concentration). It was also observed from Table 2 that higher k_{ip} values are obtained at higher dye concentrations which can be attributed to availability of enhanced driving force at higher AG 25 concentrations. Similar trend and behavior of multistep mechanism have also been reported for Acid Violet 17 dye removal using activated *Ficus racemosa* (Jain and Gogate, 2017a) and for reactive dye removal using biosorbent based on activated jujube stones (Daoud et al., 2017).

3.2.5. Effect of temperature

Fig. 8 depicts temperature effect on the variation in the sorption capacity of NAPD at equilibrium with equilibrium concentration. The obtained equilibrium curves for different temperatures were found to be steeper initially but became flat later confirming attainment of saturation of NAPD biosorbent with an increase in dye concentration. The equilibrium sorption capacity was found to increase from 44.28 mg/g at 293 K to 50.79 mg/g at 323 K. Higher sorption capacity at increased temperature is possibly attributed to the swelling within NAPD internal structure, enabling deeper penetration of AG 25 dye into NAPD pores (Babaei et al., 2016). Similar results for the effect of temperature have also been reported for Orange G dye removal using nanoclay (Salam et al., 2017).

3.2.6. Equilibrium study

Equilibrium data obtained for adsorption of AG 25 on NAPD biosorbent have also been analyzed using various isotherms such as Langmuir and Temkin.

Langmuir model is given as follows (Langmuir, 1918):

$$q_e = \frac{q_{max} K_L C_e}{1 + K_L C_e} \tag{10}$$

where q_{max} is maximum sorption capacity (mg/g) and K_L is Langmuir constant (L/mg).

Temkin model is given as follows (Temkin and Pyzhev, 1940):

$$q_e = B_T \ln(K_T C_e) \tag{11}$$

where K_T (L/mg) and B_T (mg/g) are the Temkin model constants.

Nonlinear regression analysis was performed to estimate the isotherm model constants. To compare the quality of fitting of isotherm models to the experimental data, relative error values have also been evaluated. The estimated values of R^2, isotherm constants for the models and relative error values are depicted in Table 3. R^2 values obtained for Langmuir isotherm (average value of 0.9791) were found closer to unity in comparison with R^2 values of Temkin isotherm (average value of 0.9551). The comparison of experimental and calculated values of the equilibrium sorption capacities at different conditions from isotherm models has been shown in Fig. 9. It can also be seen from Fig. 9 that calculated values of equilibrium biosorption capacity using the Langmuir isotherm are close to experimental values. Relative error values for the Langmuir isotherm were also found to be significantly less as compared to Temkin isotherm, as observed from Table 3. The obtained findings confirmed better fitting of Langmuir model to the equilibrium data as compared to Temkin isotherm. It is also important to note that as observed from Table 3, K_L values increased

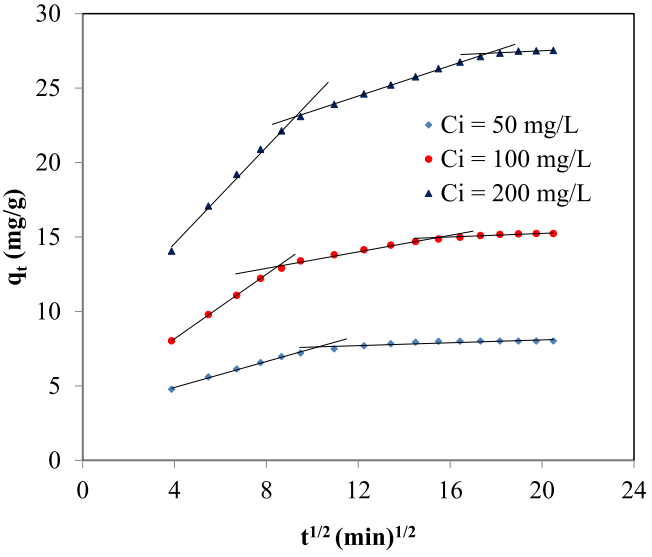

Fig. 7. Weber-Morris plot for removal of AG 25 dye using NAPD.

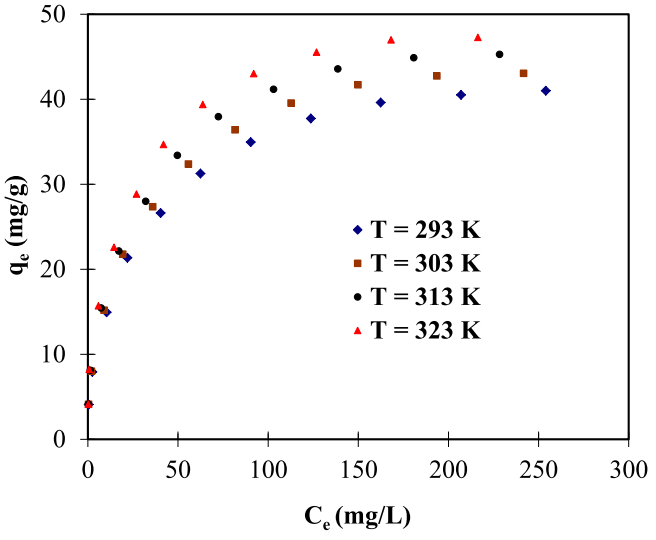

Fig. 8. Equilibrium biosorption isotherms at different temperatures for the removal of AG 25 dye using NAPD.

Table 3
Isotherm parameters for the removal of AG 25 dye using NAPD obtained for different models (t = 330 min, pH = 2, m = 6 g/L).

Isotherm model	Parameter	Values			
Langmuir	T (K)	293	303	313	323
	q_{max} (mg/g)	44.28	46.62	48.88	50.79
	K_L (L/mg)	0.044	0.047	0.050	0.058
	R^2	0.9837	0.9818	0.9774	0.9735
	Relative error	1.895	2.274	2.905	3.659
Temkin	T (K)	293	303	313	323
	B_T (mg/g)	6.66	6.81	6.86	6.89
	K_T (L/mg)	1.77	2.16	2.86	3.96
	R^2	0.9609	0.9555	0.9512	0.9526
	Relative error	9.205	15.022	18.135	13.104

from 0.044 L/mg at 293 K to 0.058 L/mg at 323 K, confirming the endothermic nature of the biosorption process.

3.2.7. Thermodynamics study

Thermodynamic parameters of biosorption such as enthalpy change (ΔH, kJ/mol), free energy change (ΔG, kJ/mol) and entropy change (ΔS, kJ/mol K) were obtained from the fitting based on the following equation:

$$lnK = -\frac{\Delta G}{RT} = -\frac{\Delta H}{R}\frac{1}{T} + \frac{\Delta S}{R} \quad (12)$$

Equilibrium constant K in above equation is a dimensionless parameter. Isotherm constants K_L and K_T (L/mg) were converted into units of L/mol and then equilibrium constant K was obtained by multiplying with the factor of 55.5, which is a molar concentration (mol/L) of water (Tran et al., 2017). The calculated parameter values after the fitting of the data are summarized in Table 4. It can be seen from Table 4 that ΔG values for all studied temperatures are negative, indicating spontaneous nature of the biosorption process (Lin et al., 2017). Positive value of ΔH (6.991 kJ/mol) confirmed endothermic nature of the biosorption process (Mella et al., 2017) as also observed earlier based on the Langmuir model parameters at different temperatures. It can be also established that as ΔH value obtained in the present study is less than 40 kJ/mol, adsorption is characterized to be physical in nature (Konicki et al., 2017). Positive ΔS value suggested an increase in randomness and excellent adsorption affinity of AG 25 on NAPD biosorbent (Goswami and Phukan, 2017).

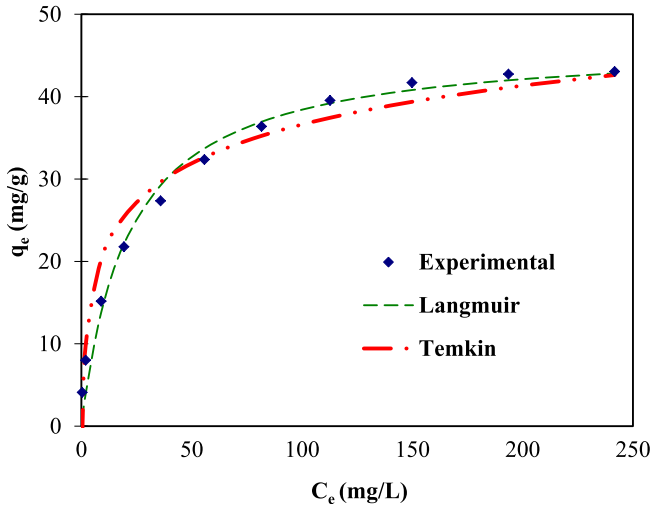

Fig. 9. Comparison of calculated adsorption capacities from different isotherms with experimental values for the removal of AG 25 using NAPD.

3.2.8. Activation energy

Activation energy for the AG 25 adsorption on NAPD in the present study has been estimated using following equation involving the second order kinetic rate constants (Tayade and Adivarekar, 2013):

$$lnk_2 = lnA - \frac{E_{act}}{RT} \quad (13)$$

Kinetic runs were performed at four different temperatures ranging from 293 to 323 K and obtained kinetic data was analyzed using pseudo second order kinetic rate equation (Equation (7)) to determine values of rate constant, k_2 and then the graph of ln k_2 against $1/T$ was plotted (Fig. 10) to evaluate activation energy, E_{act} (kJ/mol). If calculated value of E_{act} is in the range of 5–40 kJ/mol, adsorption is considered as physical adsorption and if E_{act} is in the range of 60–800 kJ/mol, adsorption is considered as chemical adsorption (Jain and Gogate, 2017b). E_{act} obtained in the present study was 6.22 kJ/mol confirming the physical nature of adsorption.

3.2.9. Comparison with other biosorbents

Table 5 shows the comparison of established values of maximum biosorption capacities (q_{max}) in the present work with q_{max} values of some of the biosorbents reported in the literature for different dyes including AG 25. It can be established from the data given in Table 5 that NaOH activated *Prunus Dulcis* biosorbent synthesized in the present work has higher value of biosorption capacity (50.79 mg/g) in comparison with the other biosorbents reported in the literature including the one obtained from *Pistacia khinjuk Stocks* and specifically applied for AG 25. The obtained results confirmed the better suitability of NaOH activated *Prunus Dulcis* biosorbent for removal of AG 25 dye from wastewater.

3.2.10. Desorption of dye and biosorbent regeneration

One of the important factors to determine feasibility of the selected adsorbent on the commercial scale is its reusability. The potential of the adsorbent for dye removal can be decided by its capacity for use in repeated cycles. Desorption experiments were conducted in a shaker on NAPD biosorbent saturated with the dye using the adsorption experiments involving 100 mg/L of AG 25 dye solution. NaOH solution of 0.1 mol/L concentration was used as a desorbing agent. The recovered NAPD biosorbent was further used for dye adsorption in repeated cycles. The obtained results for the reusability study conducted for 5 cycles have been depicted in Fig. 11. Extent of desorption (%) was observed to decrease from 98.97 to 87.68% for the 1st to 5th cycle, respectively. Biosorption capacity also decreased slightly from 15.17 mg/g for 1st cycle to 14.49 mg/g for 5th cycle. The obtained values indicated that the reusability of this biosorbent is not so good but the established trends of slight decline in biosorption capacity and desorption efficiency confirmed that NAPD biosorbent synthesized in the present work could be recovered and reused for AG 25 dye removal from wastewater with some addition of the fresh adsorbent in order to get the desired benefits of reuse and maintaining same removal efficiencies.

3.3. Column experiments

3.3.1. Effect of biosorbent height (Z)

The column experiments were conducted for different heights of biosorbent bed as 3, 4 and 5 cm by passing AG 25 dye solution with initial concentration of 100 mg/L at 8 mL/min as the flow rate and obtained breakthrough curves have been shown in Fig. 12A.

Table 4
Thermodynamic parameters for the removal of AG 25 dye using NAPD ($t = 330$ min, pH = 2, $m = 6$ g/L).

Isotherm	ΔG (kJ/mol)				ΔH (kJ/mol)	ΔS (kJ/mol K)
	293 K	303 K	313 K	323 K		
Langmuir	−34.676	−36.013	−37.384	−38.965	6.991	0.142
Temkin	−43.681	−45.671	−47.903	−50.416	21.978	0.224

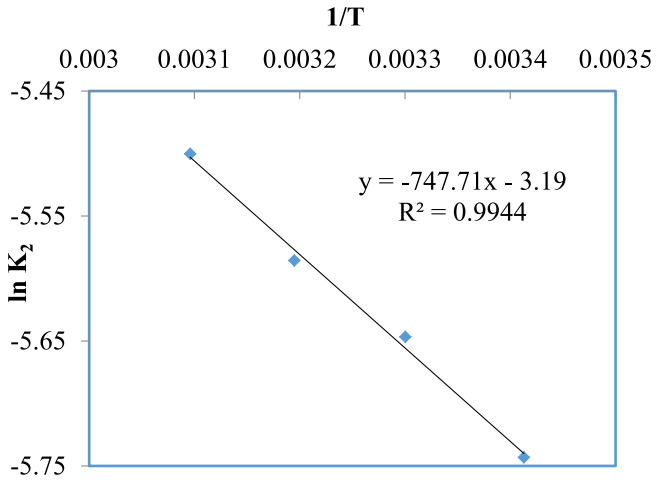

Fig. 10. Activation energy determination for the removal of AG 25 using NAPD.

The obtained results in the column operation for the different breakthrough parameters as breakthrough time (t_b), exhaustion time (t_e) and maximum uptake capacity (q_m) are depicted in Table 6. Steeper curves were obtained for lower biosorbent heights. Breakthrough time and exhaustion time was observed to increase with an increase in the biosorbent height in the column. The biosorption capacity of NAPD increased from 22.15 to 37.51 mg/g when biosorbent height in the column was increased from 3 to 5 cm. The obtained trend of larger breakthrough time, exhaustion time and biosorption capacity values at increased heights can be due to availability of more number of binding sites for the AG 25 dye adsorption as more amount of the biosorbent was available at larger heights. When height of biosorbent in the column was reduced, dye molecules did not get sufficient time to diffuse completely into the biosorbent mass, leading to lower values of biosorption capacities (Taty-costodes et al., 2005). The obtained experimental results confirmed enhanced performance of the column at larger biosorbent heights. Similar trend was also reported

Table 5
Literature reports for Maximum biosorption capacity (q_{max}) values of different biosorbents for removal of dyes from wastewater and comparison with present work.

Dyes	Biosorbents	q_{max} (mg/g)	Reference
AG 25	Natural *Prunus dulcis*	22.68	Present study
AG 25	NaOH activated *Prunus dulcis*	50.79	Present study
AG 25	*Pistacia khinjuk* Stocks	16	(Aydın and Baysal, 2006)
Acid Red 183	*Pistacia khinjuk* Stocks	33	(Aydın and Baysal, 2006)
Acid brilliant blue	Waste coir pith	16.67	(Namasivayam et al., 2001)
Methyl orange	Banana peel	21	(Annadurai et al., 2002)
Congo red	Banana peel	18.2	(Annadurai et al., 2002)
Direct blue-86	Orange peel	33.78	(Nemr et al., 2009)
Congo red	Lemon peel	34.5	(Bhatnagar et al., 2009)
Sunset yellow	Peanut hull	13.99	(Gong et al., 2005)
Reactive red 195	*Pinus sylvestris* cones	8.425	(Aksakal and Ucun, 2010)

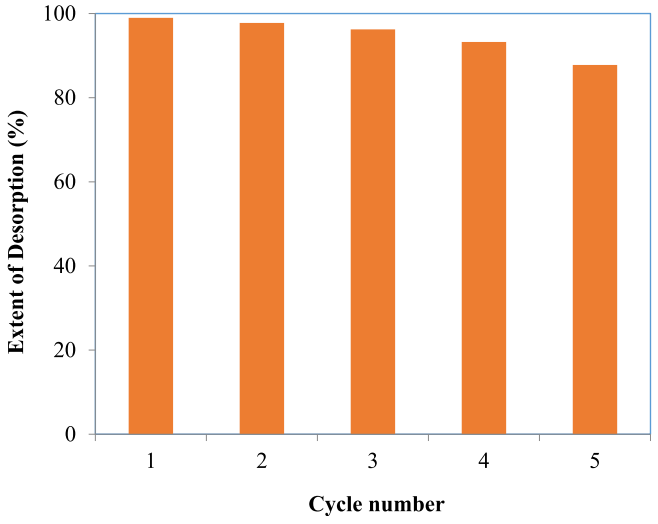

Fig. 11. Reusability study of NAPD in batch operation.

for direct deep blue dye removal using glucose carbon composite based bisorbents (Zheng et al., 2016).

3.3.2. Effect of flow rate of dye solution (Q)

The column experiments for understanding the effect of flow rate of dye solution were conducted for 4 cm height of biosorbent bed by passing AG 25 dye solution with initial concentration of 100 mg/L at different flow rates of dye solution as 6, 8 and 10 mL/min and established breakthrough curves have been shown in Fig. 12B. The obtained results for the breakthrough time (t_b), exhaustion time (t_e) and maximum uptake capacity (q_m) are also depicted in Table 6. Steeper curves were obtained for higher values of flow rates. The biosorption capacity of NAPD increased from 23.26 to 33.03 mg/g when flow rate of dye solution in the column was decreased from 10 to 6 mL/min. The obtained experimental results confirmed enhanced performance of the column at lower values of flow rate. The void fraction of the biosorbent bed was estimated as 0.146. At lower flow rate of 6 mL/min and 4 cm bed height, residence time of dye solution in the biosorbent bed was estimated to be 2.09 min. At lower flow rates, dye molecules are getting enough residence time in the column so that molecules are

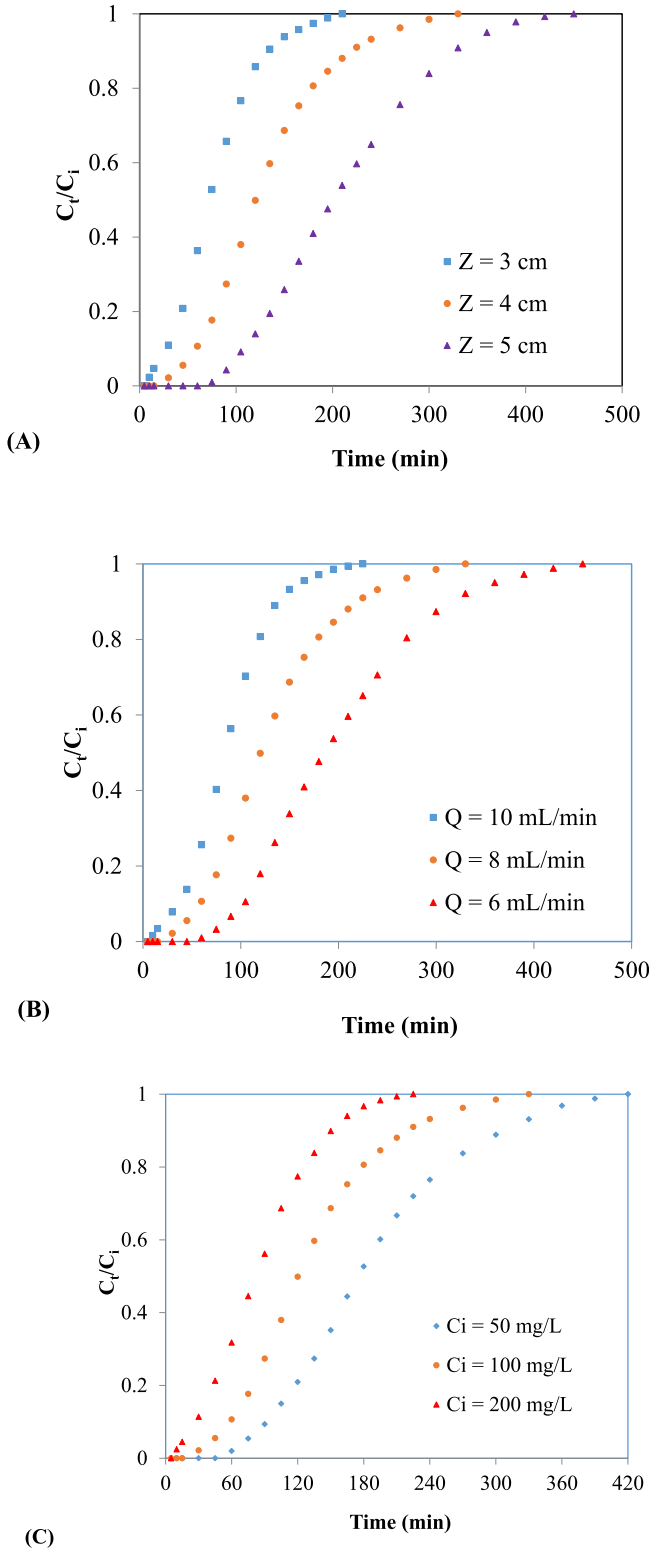

Fig. 12. Effect of column parameters on breakthrough curve for biosorption of AG 25 on NAPD A) biosorbent height B) flow rate of dye solution C) initial dye concentration.

deeply penetrated into the pores of the biosorbent whereas at higher flow rate, residence time of molecules is reduced and dye molecules are leaving the column before the establishment of equilibrium which leads to decrease in values of biosorption capacities. Similar trend of lower biosorption capacities at higher flow rate values was also reported for the Rhodamine B removal using activated *Volvariella volvacea* (Li et al., 2015).

Table 6
Breakthrough parameters for different biosorbent height (Z), flow rate of dye solution (Q) and initial dye concentration (C_i).

Z (cm)	Q (mL/min)	C_i (mg/L)	t_b (min)	t_e (min)	q_m (mg/g)
3	8	100	30	135	22.15
4	8	100	60	220	28.57
5	8	100	105	330	37.51
4	10	100	35	140	23.26
4	6	100	100	320	33.03
4	8	50	95	305	20.76
4	8	200	30	150	36.77

3.3.3. *Effect of dye concentration (C_i)*

The column experiments for understanding the effect of initial AG 25 dye concentration were conducted using 4 cm of biosorbent height by passing AG 25 dye solution having different concentrations as 50, 100 and 200 mg/L at constant 8 mL/min as the flow rate. The established breakthrough curves have been shown in Fig. 12C whereas the obtained results for the breakthrough time (t_b), exhaustion time (t_e) and maximum biosorption capacity (q_m) are depicted in Table 6. Steeper curves were obtained at higher values of initial concentrations. The biosorption capacity of NAPD increased from 20.76 to 36.77 mg/g when concentration of AG 25 dye in the solution was increased from 50 to 200 mg/L. Breakthrough time, exhaustion time and hence the volume which can be treated were observed to decrease with an increase in concentration of AG 25 dye solution. Less treated volume at larger dye concentration can be due to availability of more driving force for mass transfer, which increases dye diffusion rate within the biosorbent and saturates the active sites of the biosorbent quickly. Early saturation at higher values of dye concentration is also due to the fact that constant mass of biosorbent is available in the column for all the conditions of lower to higher dye concentration and hence early saturation occurred for higher dye concentration. Similar trend has also been reported for methylene blue dye removal using activated bituminous coal based adsorbent (Qada et al., 2006).

3.3.4. *Mathematical modeling of the column data*

In the present adsorption study, Adams–Bohart, Thomas and Yoon-Nelson model were applied for analysis of the obtained experimental data.

Adams-Bohart model is expressed as follows (Bohart and Adams, 1920):

$$\frac{C_t}{C_i} = exp\left(k_{AB}C_i t - \frac{k_{AB}N_0 Z}{U_0}\right) \tag{14}$$

where k_{AB} is Adams-Bohart kinetic constant (L mg^{-1} min^{-1}), N_0 is maximum quantity of dye adsorbed (mg) per unit volume (L) and U_0 is linear velocity of solution in the column (cm/min).

Thomas model equation is expressed as follows (Thomas, 1944):

$$\frac{C_t}{C_i} = \frac{1}{1 + exp\left(\frac{k_T q_T W}{Q} - k_T C_i t\right)} \tag{15}$$

where k_T is Thomas rate constant (mL min^{-1} mg^{-1}) and q_T is maximum biosorption capacity (mg/g).

Yoon-Nelson model is expressed as follows (Yoon and Nelson, 1984):

Table 7
Adams–Bohart, Thomas and Yoon-Nelson model parameters for the removal of AG 25 dye using NAPD.

Column operating parameters	Z (cm)	3	4	5	4	4	4	4
	Q (mL/min)	8	8	8	10	6	8	8
	C_i (mg/L)	100	100	100	100	100	50	200
Adams-Bohart parameters	$k_{AB} \times 10^5$ (L mg^{-1} min^{-1})	7.3	5.4	4.8	7.1	4.6	9.4	3.7
	N_0 (mg/L)	15,623	17,908	20,554	16,054	18,858	12,010	25,023
	R^2	0.7758	0.7549	0.8230	0.7734	0.7990	0.7955	0.8045
Thomas parameters	k_T (mL min^{-1} mg^{-1})	0.431	0.288	0.206	0.435	0.208	0.447	0.181
	q_T (mg/g)	22.85	28.51	37.37	24.22	32.65	20.52	38.11
	q_m (mg/g)	22.15	28.57	37.51	23.26	33.03	20.76	36.77
	R^2	0.9967	0.9945	0.9950	0.9990	0.9935	0.9949	0.9965
Yoon-Nelson parameters	k_Y (min^{-1})	0.0431	0.0288	0.0206	0.0435	0.0208	0.0224	0.0363
	τ (min)	75.42	125.46	205.55	85.25	191.53	180.54	83.85
	$t_{0.5}$ (min)	75	120	200	85	185	175	85
	R^2	0.9967	0.9945	0.9950	0.9990	0.9935	0.9949	0.9965

$$\frac{C_t}{C_i - C_t} = exp(k_Y t - \tau k_Y) \quad (16)$$

where k_Y is Yoon-Nelson kinetic constant (min^{-1}) and τ (min) is the time necessary to achieve 50% dye breakthrough.

Nonlinear regression analysis was performed to estimate the model parameters and the calculated parameters values for the Adams-Bohart model (N_0 and k_{AB}), Thomas model (k_T and q_T) and Yoon-Nelson model (k_Y and τ) as well as R^2 values for each fitting have been given in Table 7.

The fitting of the obtained experimental column data to different models has been compared in terms of R^2 and predicted values from the model. The R^2 values (average value 0.7894) of Adams-Bohart model were not close to 1 which revealed that Adams-Bohart model did not fit well to the obtained breakthrough curves. The R^2 values (average value of 0.9957) for the Thomas and Yoon-Nelson model were closer to 1. Also, the experimental biosorption capacity (q_m) values were observed to be also closer to biosorption capacity values calculated using the Thomas model (q_T) for all the operating column parameters as per the data given in Table 7. Time required to achieve 50% dye breakthrough obtained experimentally ($t_{0.5}$) were quite closer to that obtained by Yoon-Nelson model for all the operating column parameters as observed from Table 7. All these findings confirmed that Thomas and Yoon-Nelson model fitted well to the obtained breakthrough data.

3.3.5. Column reusability study

In the present study, used adsorbent was regenerated by passing 0.1 mol/L of NaOH solution through the column as a desorbing agent at the flow rate of 8 mL/min. Maximum dye desorption for was observed to be occurred in 30 min of treatment for all the 5 cycles of regeneration. During the subsequent reuse, the biosorption capacity of NAPD biosorbent was found to marginally decrease from 28.57 mg/g for 1st cycle to 25.19 mg/g for 5th cycle of reuse. The obtained results established that NAPD biosorbent synthesized in the present work can be used repeatedly in the column to adsorb AG 25 dye with a small decrease in biosorption capacity, which can be compensated by using some fresh adsorbent mixed with the regenerated adsorbent. The performed reusability study confirmed potential of NAPD biosorbent to adsorb AG 25 dye from wastewater in repeated cycles with some adjustment in operation.

4. Conclusions

The present study focused on the biosorbent synthesis from the fallen leaves of *Prunus Dulcis* with activation using NAOH and its application for removal of Acid Green 25 dye from aqueous solution in batch and column operation. The maximum equilibrium biosorption capacity in batch mode was estimated as 50.79 mg/g at pH of 2, loading of activated biosorbent as 6 g/L and temperature of 323 K. Pseudo second order and Langmuir isotherm were established to give better fitting to the obtained experimental data whereas the column data in terms of the breakthrough parameters was observed to be well described by Thomas and Yoon-Nelson model. The regeneration and reuse study confirmed better utilization of synthesized biosorbent for five cycles in both batch and column operation with slight decrease in biosorption capacity, which can be compensated with some operational modifications. The work has conclusively established the potential of activated biosorbent to effectively treat the dye containing wastewater.

Acknowledgements

The authors express their gratitude to the University Grants Commission, India for the support under the scheme of Networking Resource Centre in Chemical Engineering.

References

Adegoke, K.A., Bello, O.S., 2015. Dye sequestration using agricultural wastes as adsorbents. Water Resour. Ind. 12, 8–24.
Aksakal, O., Ucun, H., 2010. Equilibrium, kinetic and thermodynamic studies of the biosorption of textile dye (Reactive Red 195) onto *Pinus sylvestris* L. J. Hazard. Mater. 181, 666–672.
Almasian, A., Najafi, F., Mirjalili, M., Gashti, M.P., Fard, G.C., 2016. Zwitter ionic modification of cobalt-ferrite nanofiber for the removal of anionic and cationic dyes. J. Taiwan Inst. Chem. Eng. 67, 306–317.
Annadurai, G., Juang, R., Lee, D., 2002. Use of cellulose-based wastes for adsorption of dyes from aqueous solutions. J. Hazard. Mater. 92, 263–274.
Ayad, M.M., El-Nasr, A.A., 2012. Anionic dye (acid green 25) adsorption from water by using polyaniline nanotubes salt/silica composite. J. Nanostruct. Chem. 3, 1–9.
Aydın, H., Baysal, G., 2006. Adsorption of acid dyes in aqueous solutions by shells of bittim (*Pistacia khinjuk* Stocks). Desalination 196, 248–259.
Babaei, A.A., Khataee, A., Ahmadpour, E., Sheydaei, M., Kakavandi, B., Alaee, Z., 2016. Optimization of cationic dye adsorption on activated spent tea: equilibrium, kinetics, thermodynamic and artificial neural network modeling. Kor. J. Chem. Eng. 33, 1352–1361.
Balla, W., Essadki, A.H., Gourich, B., Dassaa, A., Chenik, H., Azzi, M., 2010. Electrocoagulation/electroflotation of reactive, disperse and mixture dyes in an external-loop airlift reactor. J. Hazard. Mater. 184, 710–716.
Banerjee, S., Chattopadhyaya, M.C., 2017. Adsorption characteristics for the removal of a toxic dye, tartrazine from aqueous solutions by a low cost agricultural by-product. Arab. J. Chem. 10, S1629–S1638.
Belbachir, I., Makhoukhi, B., 2017. Adsorption of Bezathren dyes onto sodic bentonite from aqueous solutions. J. Taiwan Inst. Chem. Eng. 75, 105–111.
Bensalah, H., Bekheet, M.F., Younssi, S.A., Ouammou, M., Gurlo, A., 2017. Removal of cationic and anionic textile dyes with moroccan natural phosphate. J. Environ. Chem. Eng. 5, 2189–2199.
Bharathi, K.S., Ramesh, S.T., 2013. Removal of dyes using agricultural waste as low-cost adsorbents: a review. Appl. Water Sci. 3, 773–790.
Bhatnagar, A., Kumar, E., Minocha, A.K., Jeon, B., Song, H., Seo, Y., 2009. Removal of anionic dyes from water using *Citrus limonum* (lemon) peel: equilibrium studies

and kinetic modeling. Sep. Sci. Technol. 44, 316–334.
Bhattacharyya, A., Mondal, D., Roy, I., Sarkar, G., Saha, N.R., Rana, D., Ghosh, T.K., Mandal, D., Chakraborty, M., Chattopadhyay, D., 2017. Studies of the kinetics and mechanism of the removal process of Proflavine dye through adsorption by graphene oxide. J. Mol. Liq. 230, 696–704.
Bohart, G.S., Adams, E.Q., 1920. Some aspects of the behavior of charcoal with respect to chlorine. J. Am. Chem. Soc. 42, 523–544.
Chowdhury, S., Chakraborty, S., Saha, P., 2011. Biosorption of Basic Green 4 from aqueous solution by *Ananas comosus* (pineapple) leaf powder. Colloids Surf. B Biointerfaces 84, 520–527.
Dahri, M.K., Lim, L.B.L., Kooh, M.R.R., Chan, C.M., 2017. Adsorption of brilliant green from aqueous solution by unmodified and chemically modified Tarap (*Artocarpus odoratissimus*) peel. Int. J. Environ. Sci. Technol. 14, 2683–2694.
Daoud, M., Benturki, O., Kecira, Z., Girods, P., Donnot, A., 2017. Removal of reactive dye (BEZAKTIV Red S-MAX) from aqueous solution by adsorption onto activated carbons prepared from date palm rachis and jujube stones. J. Mol. Liq. 243, 799–809.
Demirbas, A., 2009. Agricultural based activated carbons for the removal of dyes from aqueous solutions: a review. J. Hazard. Mater. 167, 1–9.
Gong, R., Ding, Y., Li, M., Yang, C., Liu, H., Sun, Y., 2005. Utilization of powdered peanut hull as biosorbent for removal of anionic dyes from aqueous solution. Dyes Pigments 64, 187–192.
Goswami, M., Phukan, P., 2017. Enhanced adsorption of cationic dyes using sulfonic acid modified activated carbon. J. Environ. Chem. Eng. 5, 3508–3517.
Gündüz, F., Bayrak, B., 2017. Biosorption of malachite green from an aqueous solution using pomegranate peel: equilibrium modelling, kinetic and thermodynamic studies. J. Mol. Liq. 243, 790–798.
Guo, J., Chen, S., Liu, L., Li, B., Yang, P., Zhang, L., Feng, Y., 2012. Adsorption of dye from wastewater using chitosan–CTAB modified bentonites. J. Colloid Interface Sci. 382, 61–66.
Hameed, B.H., Ahmad, A.A., Aziz, N., 2007. Isotherms, kinetics and thermodynamics of acid dye adsorption on activated palm ash. Chem. Eng. J. 133, 195–203.
Ho, Y.S., Mckay, G., 1999. Pseudo-second order model for sorption processes. Process Biochem. 34, 451–465.
Inyinbor, A.A., Adekola, F.A., Olatunji, G.A., 2016. Kinetics, isotherms and thermodynamic modeling of liquid phase adsorption of Rhodamine B dye onto *Raphia hookerie* fruit epicarp. Water Resour. Ind. 15, 14–27.
Islam, M.A., Ahmed, M.J., Khanday, W.A., Asif, M., Hameed, B.H., 2017. Mesoporous activated coconut shell-derived hydrochar prepared via hydrothermal carbonization-NaOH activation for methylene blue adsorption. J. Environ. Manag. 203, 237–244.
Jain, S.N., Gogate, P.R., 2017. NaOH-treated dead leaves of *Ficus racemosa* as an efficient biosorbent for Acid Blue 25 removal. Int. J. Environ. Sci. Technol. 14, 531–542.
Jain, S.N., Gogate, P.R., 2017a. Adsorptive removal of acid violet 17 dye from wastewater using biosorbent obtained from NaOH and H_2SO_4 activation of fallen leaves of *Ficus racemosa*. J. Mol. Liq. 243, 132–143.
Jain, S.N., Gogate, P.R., 2017b. Acid Blue 113 removal from aqueous solution using novel biosorbent based on NaOH treated and surfactant modified fallen leaves of *Prunus Dulcis*. J. Environ. Chem. Eng. 5, 3384–3394.
Jia, Z., Li, Z., Ni, T., Li, S., 2017. Adsorption of low-cost absorption materials based on biomass (*Cortaderia selloana* flower spikes) for dye removal: kinetics, isotherms and thermodynamic studies. J. Mol. Liq. 229, 285–292.
Khamparia, S., Jaspal, D.K., 2017. *Xanthium strumarium* L. seed hull as a zero cost alternative for Rhodamine B dye removal. J. Environ. Manag. 197, 498–506.
Konicki, W., Aleksandrzak, M., Mijowska, E., 2017. Equilibrium, kinetic and thermodynamic studies on adsorption of cationic dyes from aqueous solutions using graphene oxide. Chem. Eng. Res. Des. 123, 35–49.
Lagergren, S., 1898. About the theory of so called adsorption of soluble substances. Ksver Veterskapsakad Handl 24, 1–6.
Langmuir, I., 1918. The adsorption of gases on plane surfaces of glass, mica and platinum. J. Am. Chem. Soc. 40, 1361–1403.
Li, Q., Tang, X., Sun, Y., Wang, Y., Long, Y., Jiang, J., Xu, H., 2015. Removal of Rhodamine B from wastewater by modified *Volvariella volvacea*: batch and column study. RSC Adv. 5, 25337–25347.
Lin, X., Huang, Q., Qi, G., Xiong, L., Huang, C., Chen, X., Li, H., Chen, X., 2017. Adsorption behavior of levulinic acid onto microporous hyper-cross-linked polymers in aqueous solution: equilibrium, thermodynamic, kinetic simulation and fixed-bed column studies. Chemosphere 171, 231–239.
Ma, D., Zhu, B., Cao, B., Wang, J., Zhang, J., 2017. Fabrication of the novel hydrogel based on waste corn stalk for removal of methylene blue dye from aqueous solution. Appl. Surf. Sci. 422, 944–952.
Mall, I.D., Srivastava, V.C., Agarwal, N.K., Mishra, I.M., 2005. Removal of Congo red from aqueous solution by bagasse fly ash and activated carbon: kinetic study and equilibrium isotherm analyses. Chemosphere 61, 492–501.
Mella, B., Puchana-Rosero, M.J., Costa, D.E.S., Gutterres, M., 2017. Utilization of tannery solid waste as an alternative biosorbent for acid dyes in wastewater treatment. J. Mol. Liq. 242, 137–145.
Mirzaei, N., Ghaffari, H.R., Sharafi, K., Velayati, A., Hoseindoost, G., Rezaei, S., Mahvi, A.H., Azari, A., Dindarloo, K., 2017. Modified natural zeolite using ammonium quaternary based material for Acid red 18 removal from aqueous solution. J. Environ. Chem. Eng. 5, 3151–3160.
Monteiro, M.S., Farias, R.F. De, Chaves, J.A.P., Santana, S.A., Silva, H.A.S., Bezerra, C.W.B., 2017. Wood (Bagassa *guianensis Aubl*) and green coconut mesocarp (*cocos nucifera*) residues as textile dye removers (Remazol Red and Remazol Brilliant Violet). J. Environ. Manag. 204, 23–30.
Moussavi, G., Khosravi, R., 2011. The removal of cationic dyes from aqueous solutions by adsorption onto pistachio hull waste. Chem. Eng. Res. Des. 89, 2182–2189.
Namasivayam, C., Dinesh Kumar, M., Selvi, K., Ashruffunissa Begum, R., Vanathi, T., Yamuna, R.T., 2001. 'Waste' coir pith - a potential biomass for the treatment of dyeing wastewaters. Biomass Bioenergy 21, 477–483.
Nataraj, S.K., Hosamani, K.M., Aminabhavi, T.M., 2009. Nanofiltration and reverse osmosis thin film composite membrane module for the removal of dye and salts from the simulated mixtures. Desalination 249, 12–17.
Nemr, A. El, Abdelwahab, O., El-Sikaily, A., Khaled, A., 2009. Removal of direct blue-86 from aqueous solution by new activated carbon developed from orange peel. J. Hazard. Mater. 161, 102–110.
Ng, H.K.M., Leo, C.P., Abdullah, A.Z., 2017. Selective removal of dyes by molecular imprinted TiO_2 nanoparticles in polysulfone ultrafiltration membrane. J. Environ. Chem. Eng. 5, 3991–3998.
Ngulube, T., Gumbo, J.R., Masindi, V., Maity, A., 2017. An update on synthetic dyes adsorption onto clay based minerals: a state-of-art review. J. Environ. Manag. 191, 35–57.
Ozacar, M., Ayhan Sengil, I., 2005. Adsorption of metal complex dyes from aqueous solutions by pine sawdust. Bioresour. Technol. 96, 791–795.
Ozcan, A., Ozcan, A.S., 2005. Adsorption of Acid Red 57 from aqueous solutions onto surfactant-modified sepiolite. J. Hazard. Mater. 125, 252–259.
Pachhade, K., Sandhya, S., Swaminathan, K., 2009. Ozonation of reactive dye, Procion red MX-5B catalyzed by metal ions. J. Hazard. Mater. 167, 313–318.
Pereira, F.A.R., Sousa, K.S., Cavalcanti, G.R.S., França, D.B., Queiroga, L.N.F., Santos, I.M.G., Fonseca, M.G., Jaber, M., 2017. Green biosorbents based on chitosan-montmorillonite beads for anionic dye removal. J. Environ. Chem. Eng. 5, 3309–3318.
Prahas, D., Kartika, Y., Indraswati, N., Ismadji, S., 2008. Activated carbon from jackfruit peel waste by H3PO4 chemical activation: pore structure and surface chemistry characterization. Chem. Eng. J. 140, 32–42.
Preethi, S., Sivasamy, A., Sivanesan, S., Ramamurthi, V., Swaminathan, G., 2006. Removal of safranin basic dye from aqueous solutions by adsorption onto corncob activated carbon. Ind. Eng. Chem. Res. 45, 7627–7632.
Qada, E.N. El, Allen, S.J., Walker, G.M., 2006. Adsorption of basic dyes onto activated carbon using microcolumns. Ind. Eng. Chem. Res. 45, 6044–6049.
Salam, M.A., Kosa, S.A., Al-beladi, A.A., 2017. Application of nanoclay for the adsorptive removal of Orange G dye from aqueous solution. J. Mol. Liq. 241, 469–477.
Santos, R.M.M. dos, Goncalves, R.G.L., Constantino, V.R.L., Santilli, C.V., Borges, P.D., Tronto, J., Pinto, F.G., 2017. Adsorption of Acid Yellow 42 dye on calcined layered double hydroxide: effect of time, concentration, pH and temperature. Appl. Clay Sci. 140, 132–139.
Shakoor, S., Nasar, A., 2017. Adsorptive treatment of hazardous methylene blue dye from artificially contaminated water using *cucumis sativus* peel waste as a low-cost adsorbent. Groundw. Sustain. Dev. 5, 152–159.
Shi, Q., Zhang, J., Zhang, C., Li, C., Zhang, B., Hu, W., Xu, J., Zhao, R., 2010. Preparation of activated carbon from cattail and its application for dyes removal. J. Environ. Sci. 22, 91–97.
Sidiras, D., Batzias, F., Schroeder, E., Ranjan, R., Tsapatsis, M., 2011. Dye adsorption on autohydrolyzed pine sawdust in batch and fixed-bed systems. Chem. Eng. J. 171, 883–896.
Singh, D.K., Kumar, V., Mohan, S., Bano, D., Hasan, S.H., 2017a. Breakthrough curve modeling of graphene oxide aerogel packed fixed bed column for the removal of Cr(VI) from water. J. Water Process Eng. 18, 150–158.
Singh, H., Chauhan, G., Jain, A.K., Sharma, S.K., 2017b. Adsorptive potential of agricultural wastes for removal of dyes from aqueous solutions. J. Environ. Chem. Eng. 5, 122–135.
Singh, S.A., Shukla, S.R., 2016. Adsorptive removal of cobalt ions on raw and alkali-treated lemon peels. Int. J. Environ. Sci. Technol. 13, 165–178.
Singh, S., Lo, S.L., Srivastav, V.C., Hiwarkar, A.D., 2016. Comparative study of electrochemical oxidation for dye degradation: parametric optimization and mechanism identification. J. Environ. Chem. Eng. 4, 2911–2921.
Song, K., Xu, H., Xu, L., Xie, K., Yang, Y., 2017. Preparation of cellulose nanocrystal-reinforced keratin bioadsorbent for highly effective and recyclable removal of dyes from aqueous solution. Bioresour. Technol. 232, 254–262.
Souza, S.M.A.G.U. de, Peruzzo, L.C., Souza, A.A.U. de, 2008. Numerical study of the adsorption of dyes from textile effluents. Appl. Math. Model. 32, 1711–1718.
Srivastava, V.C., Mall, I.D., Mishra, I.M., 2007. Adsorption thermodynamics and isosteric heat of adsorption of toxic metal ions onto bagasse fly ash (BFA) and rice husk ash (RHA). Chem. Eng. J. 132, 267–278.
Subramaniam, R., Ponnusamy, S.K., 2015. Novel adsorbent from agricultural waste (cashew NUT shell) for methylene blue dye removal: optimization by response surface methodology. Water Resour. Ind. 11, 64–70.
Tangaraj, V., Janot, J., Jaber, M., Bechelany, M., Balme, S., 2017. Adsorption and photophysical properties of fluorescent dyes over montmorillonite and saponite modified by surfactant. Chemosphere 184, 1355–1361.
Taty-costodes, V.C., Fauduet, H., Porte, C., Ho, Y., 2005. Removal of lead (II) ions from synthetic and real effluents using immobilized Pinus sylvestris sawdust: adsorption on a fixed-bed column. J. Hazard. Mater. 123, 135–144.
Tayade, P.B., Adivarekar, R.V., 2013. Adsorption kinetics and thermodynamic study of *Cuminum cyminum* L. dyeing on silk. J. Environ. Chem. Eng 1, 1336–1340.
Temkin, M.J., Pyzhev, V., 1940. Recent modifications to Langmuir isotherms. Acta Physicochim. USSR 12, 217–225.

Thomas, H.C., 1944. Heterogeneous ion exchange in a flowing system. J. Am. Chem. Soc. 66, 1664–1666.
Tran, H.N., You, S.J., Hosseini, B.,A., Chao, H.P., 2017. Mistakes and inconsistencies regarding adsorption of contaminants from aqueous solutions: a critical review. Water Res. 120, 88–116.
Weber, W.J., Carrell Morris, J., 1963. Kinetics of adsorption on carbon from solution. J. Sanit. Eng. Div. Am. Soc. Civ. Eng. 89, 31–60.
Wu, X., Wu, D., Fu, R., Zeng, W., 2012. Preparation of carbon aerogels with different pore structures and their fixed bed adsorption properties for dye removal. Dyes Pigments 95, 689–694.
Wu, Y., Zhang, W., Yu, W., Liu, H., Chen, R., Wei, Y., 2015. Ferrihydrite preparation and its application for removal of anionic dyes. Front. Environ. Sci. Eng. 9, 411–418.
Xue, C., Chen, Q., Liu, Y., Yang, Y., Xu, D., Xue, L., Zhang, W., 2015. Acid blue 9 desalting using electrodialysis. J. Membr. Sci. 493, 28–36.
Yoon, Y.H., Nelson, J.H., 1984. Application of gas adsorption kinetics I. A theoretical model for respirator cartridge service life. Am. Ind. Hyg. Assoc. J. 45, 509–516.
Yusuf, M., Khan, M.A., Otero, M., Abdullah, E.C., Hosomi, M., Terada, A., Riya, S., 2017. Synthesis of CTAB intercalated graphene and its application for the adsorption of AR265 and AO7 dyes from water. J. Colloid Interface Sci. 493, 51–61.
Zeng, G., Ye, Z., He, Y., Yang, X., Ma, J., Shi, H., Feng, Z., 2017. Application of dopamine-modified halloysite nanotubes/PVDF blend membranes for direct dyes removal from wastewater. Chem. Eng. J. 323, 572–583.
Zheng, P., Bai, B., Guan, W., Wang, H., Suo, Y., 2016. Fixed-bed column studies for the removal of anionic dye from aqueous solution using TiO_2 @ glucose carbon composites and bed regeneration study. J. Mater. Sci. Mater. Electron. 27, 867–877.
Zhou, Y., Zhang, L., Cheng, Z., 2015. Removal of organic pollutants from aqueous solution using agricultural wastes: a review. J. Mol. Liq. 212, 739–762.